

Microwave-Hydrothermal Synthesis and Hyperfine Characterization of Praseodymium-Doped Nanometric Zirconia Powders

Federica Bondioli,[†] Cristina Leonelli, and Tiziano Manfredini

Dipartimento di Ingegneria dei Materiali e dell'Ambiente, Università di Modena e Reggio Emilia, 41100 Modena, Italy

Anna Maria Ferrari

Dipartimento di Scienze e Metodi dell'Ingegneria, Università di Modena e Reggio Emilia, 42100 Reggio Emilia, Italy

Maria Cristina Caracoche,* Patricia Claudia Rivas,** and Agustín Mario Rodríguez**

Departamento de Física, Universidad Nacional de La Plata, 1900 La Plata, Argentina

This work focuses on the microwave-assisted hydrothermal synthesis of praseodymium-doped zirconia and on the subsequent evaluation of the effect of synthesis conditions on powder properties. Pure and 10 mol% Pr-doped zirconia samples have been analyzed by X-ray diffraction (XRD) and the perturbed angular correlations hyperfine technique, which probes the nearest environments of zirconium ions. At atomic scale, as determined from perturbed angular correlation data, the XRD amorphous fraction of the as-obtained powders exhibits a tetragonal-like structure. The pure powder becomes partially stabilized and the doped powder is a substitutional solid solution of praseodymium in tetragonal zirconia.

I. Introduction

THERE has been an increasing trend toward the use of finer powders in ceramic processing. A growing demand for improved performance of ceramics in load-bearing applications and in functional application has raised the importance of chemical purification and processing of the starting powders. Maximum control of a ceramic process begins with the starting material and powder preparation. Consequently, numerous chemical unconventional preparation methods that include forced hydrolysis, urea-based homogeneous precipitation, coprecipitation, hydrothermal synthesis, flux method, reaction in microemulsion, and sol-gel synthesis,¹ likely to lead to suitable powders, have been extensively investigated.

Among the different methods, the hydrothermal crystallization^{2–4} is an interesting process to directly prepare nanometer-sized crystalline powders with reduced contamination and low synthesis temperature. A late innovation to the hydrothermal method, developed by Komarneni *et al.*,^{5–7} involves the introduction of microwave during the hydrothermal synthesis to increase the kinetics of crystallization by one to two orders of magnitude and sometimes to lead to novel phases. As it has been recently reported,⁸ the microwave application is an efficient way to enhance powder crystallinity and decrease processing times. In particular, in a previous work, the authors have demonstrat-

ed that it is possible to obtain a metastable tetragonal *t'*-phase of ZrO₂ at room temperature under microwave-assisted hydrothermal conditions starting from ZrOCl₂ 1M and NaOH 0.5M.⁹

It is well known that zirconia is a typical polymorphic material that may exist in monoclinic (*m*), tetragonal (*t*), and cubic (*c*) crystalline forms at different temperatures.¹⁰ However, the phase formation and the transformation behavior of hydrous-zirconia powders are affected by various synthesis conditions or processing parameters¹¹ and, thus, may not always follow the traditional phase transition route. Studies on new dopant agents capable of producing zirconia-based powders with improved physical and chemical properties are still of great interest. Doping of Me(III) oxides leads to both an increase in the oxygen vacancy concentration and an enhancement of the oxygen-ion conductivity, which enables to use these stabilized zirconia as an electrolyte in the fuel cells. The purpose of the present work is to report the synthesis of ultrafine Pr-doped ZrO₂ powders under microwave-assisted hydrothermal conditions and the effect of the praseodymium ion on the zirconia phase stabilization. Praseodymium dopant has been chosen because it is one of the elements under investigation in the field of oxygen storage materials and it undergoes oxygen exchange at a lower temperature than cerium oxide¹² and its oxygen storage capacity is not diminished by high sintering temperature.¹³

The possibility of PrO_x-ZrO₂ solid solution formation has been hypothesized, the phase diagram being unknown, on the basis of the lanthania-zirconia phase diagram and by considering the ionic radii of Zr⁴⁺ (0.87 Å) and both Pr³⁺ (1.126 Å) and Pr⁴⁺ (0.90 Å). Previous studies of the authors¹⁴ have showed, in the 20°–1200°C thermal range, the solubility of praseodymium ion in the tetragonal zirconia structure.

The study focuses on the preparation and characterization of the pure and Pr-doped (Pr = 10 mol%) zirconia powders. In particular, in order to evaluate the metastable zirconia phases present in the samples, the perturbed angular correlation (PAC) spectroscopy has been used. The PAC method has proved to be an efficient tool in the investigation of zirconia-based ceramics at an atomic level,^{15–19} since it allows the determination of different atomic configurations around zirconium sites hardly resolvable by other techniques, which could help in explaining the ceramic bulk properties and their thermal evolution. In fact, the impurities of hafnium (1–5%) always existing in natural zirconium, randomly distributed at substitutional zirconium sites, constitute the hyperfine probes of the technique. The thermal neutron irradiation of the samples activates some ¹⁸⁰Hf isotopes by transforming them in the ¹⁸¹Hf probes.

The method briefly consists in an inspection of the angular correlation of two energetic photons emitted in succession by the radioactive nucleus ¹⁸¹Hf through the 133–482 keV disintegra-

S.-I. Hirano—contributing editor

Manuscript No. 186893. Received June 19, 2002; approved January 26, 2004.

Supported by MURST-PRIN Contract, "Application of the microwave technology to physical-chemical processing involving solids—1999–2000".

Partially supported by Comisión de Investigaciones Científicas de la Provincia de Buenos Aires and CONICET, Argentina.

*Member of CICPBA, Argentina.

**Member of CONICET, Argentina.

[†]Author to whom correspondence should be addressed. e-mail: fedebond@unimo.it

tion γ - γ cascade. The comparison of the measured angular correlation against that of the isolated probe, known from the nuclear physics, allows to gather information about the electric field gradients (EFGs) existing in the lattice where the nuclear probes Hf(Zr) are immersed. The information is drawn from the determination of the so-called quadrupole parameters that describe the EFG at the zirconium site, i.e. its intensity (through the quadrupole frequency ω_Q), its departure from axial symmetry (through the asymmetry parameter η), and its degree of disorder due to the presence of impurities or defects in the lattice (through the broadening or spread δ of the EFG). All of them can be derived from the fitting of the experimental spin rotation curves obtained at the laboratory. In addition, due to the extremely localized nature of the technique, non-equivalent sites in the lattice can be distinguished through their relative abundances f . Even small changes as single-atom relaxations, vacancies, and point defects can be detected as a modification of the particular hyperfine fingerprint corresponding to each of the zirconia polymorphs. A good example of the PAC high sensitivity is the find that both tetragonal¹⁵⁻¹⁸ and cubic¹⁹ yttria-doped zirconia metastable phases were described by a two-component hyperfine interaction involving zirconium surroundings, each distorting the lattice structure to a different extent. In the case of the tetragonal structure, one of the interactions describes the regular, eight oxygen-coordinated zirconium sites, denoted hereinafter as t -form on account of its similitude with the zirconium surroundings composing the crystalline equilibrium tetragonal phase. The other one describes the highly disordered, oxygen-defective zirconium surroundings due to the existence of structural oxygen vacancies and/or defects derived from the preparation method. It exhibits a lower tetragonality and is denoted as t' -form. As it has already been reported,¹⁸ the PAC patterns of both metastable configurations around zirconium are quite distinguishable and also different from those of the equilibrium tetragonal phase. The hyperfine parameters characterizing the various tetragonal atomic configurations are the following: $\omega_Q = 165$ Mrad/s, $\eta \cong 0.55$, and $\delta \geq 25\%$ for metastable t' -form; $\omega_Q = 185$ Mrad/s, $\eta \cong 0.2$, and $\delta \leq 2\%$ for metastable t -form and $\omega_Q = 160$ Mrad/s (at 1150°C), $\eta \leq 0.2$, and $\delta \leq 2\%$ for the equilibrium t -phase.

II. Experimental Procedure

(1) Sample Preparation

The microwave-assisted hydrothermal synthesis of ZrO₂ powders was conducted starting from ZrOCl₂·8H₂O (0.5M) aqueous solutions. Praseodymium was added as nitrate salt (Pr(NO₃)₃) in order to prepare the doped samples. Both solutions were neutralized with NaOH (1M) to pH 9. The suspensions were then treated in a Teflon-lined vessel using a microwave digestion system (Model MDS-2000, CEM, Matthews, NC). This system uses 2.45 GHz microwaves and is controlled by pressure. It can attain a maximum pressure of 14 atm. The reaction vessel was connected to a pressure transducer that monitors and controls the pressure during synthesis.

After preliminary tests, microwave-hydrothermal treatments were conducted at 14 atm for 2 h. Time, pressure, and power were computer-controlled. The power level was automatically adjusted to the required pressure. After the synthesis reaction, the pure and doped powders were filtered by centrifugation, washed, and dried in an electric furnace at 120°C for 12 h. To evaluate the presence of Na and Cl and thus the efficacy of the washing step, the supernatant was analyzed by ICP spectroscopy (Model Liberty 200, Variant, Sydney, Australia). In particular, the absence of alkali and chlorine ions in the last washing water indicated the efficacy of the washing step.

(2) Powder Characterization

To investigate the structure and crystallinity of the samples, the synthesized products were analyzed with a computer-assisted X-ray (CuK α) powder diffractometer (Model PW3710, Philips

Research Laboratories, Eindhoven, the Netherlands). The X-ray diffraction (XRD) patterns were collected in a 2θ range of 25°–90° at room temperature, with a scanning rate of 0.005°/s and a step size of 0.02°. Lattice parameters of monoclinic [P2₁/a]²⁰ and tetragonal [P4₂/nmc]²¹ phases, as well as their quantity, were determined by the combined Rietveld and reference intensity ratio (RIR) methods using GSAS.^{22,23} A 10 wt% of corundum (NIST SRM676) has been added to all samples as an internal standard. The mixtures, ground in an agate mortar, have been side loaded in an aluminum flat holder in order to minimize the preferred orientation problems. Data have been recorded in the 5°–140° 2θ range (step size 0.02° and 6 s counting time for each step). The phase fractions extracted by the Rietveld–RIR refinements have been rescaled on the basis of the absolute weight of corundum originally added to the mixtures as an internal standard, and therefore internally renormalized.

The average crystallite size was calculated using the Sherrer's formula from the width of the XRD lines.²⁴ The thermal stability of the powders up to 1200°C was evaluated by thermogravimetric and differential thermal analysis (TG-DTA) (Model 404, Netzsch, Selb, Germany) and a heating rate of 10°/min. The sample morphology and microstructure were examined by transmission electron microscopy (TEM) (Model EM400, Philips Research Laboratories). Specimens were prepared by dispersing the as-obtained powder in distilled water and then placing a drop of the suspension on a copper grid coated with a transparent polymer and then dried. The grain size distribution was determined from TEM images. The maximum diameters of more than 100 particles in TEM micrographs were measured. The surface area analysis was carried out on the as-prepared powders by BET (Model Gemini 2360, Micromeritics Instrument, Norcross, GA), using nitrogen as an adsorbate. The grain size was also calculated using the specific surface area data, by the equation:

$$\phi = \frac{6}{S\rho}$$

where ϕ is the average diameter of a spherical particle, S is the surface area of a powder, and ρ is the experimental density value of powder measured by a He picnometer (Model Accupic 1330, Micromeritics Instrument).

Regarding the PAC experiments, the samples were encapsulated in air at atmospheric pressure in 0.5 cm³ sealed quartz tubes and then irradiated with a flux of about 10¹³ neutrons·cm⁻²·s during 24 h in order to achieve the desired activity (about 100 μ Ci) of ¹⁸¹Hf. Measurements were carried out using two BaF₂ detectors in a planar arrangement. Each one lasted about 2 days and was performed in air at atmospheric pressure at increasing temperatures up to 600°C for the pure sample and up to 1150°C for the doped one. A final measurement at room temperature was taken for the doped sample. Details of the setup, data acquisition, and data handling are given elsewhere.¹⁶

III. Results

(1) Pure Zirconia (Zr0)

To investigate the nature of the as-obtained powder, the sample was subjected to XRD analysis. Figure 1 clearly indicates that the as-synthesized sample is partially stabilized: although predominantly monoclinic, peaks corresponding to the tetragonal ZrO₂ phases are also present. In spite of that fact that an unambiguous determination between the possible tetragonal crystal structures could not be made from XRD results solely since their reflections overlap, the relative intensity of the monoclinic, tetragonal, and amorphous phase has been calculated by Rietveld–RIR (see Table I). Table II reports the XRD-derived average crystallite size for the tetragonal and monoclinic structures and the interplanar spacing d for the tetragonal phase using the (111) main diffraction line. Also included is the grain size

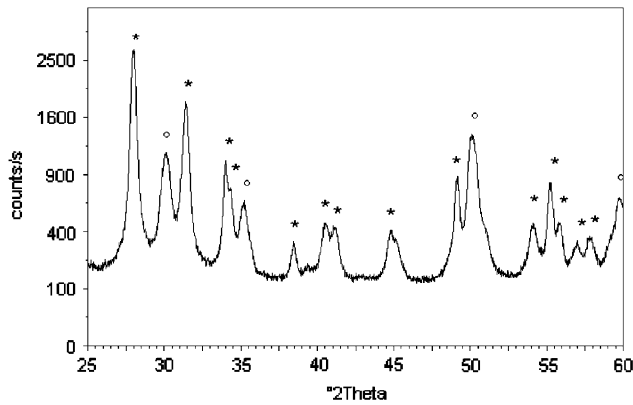


Fig. 1. X-ray diffraction pattern of as-obtained Zr0 sample. *, *m*-ZrO₂; °, *t*-ZrO₂.

Table I. Quantitative Analysis Results and Standard Rietveld Agreement Factors Obtained for Zr0 and Zr10 Samples

Phases	Samples	
	Zr0	Zr10
<i>m</i> -ZrO ₂	36.6 (4)	—
<i>t</i> -ZrO ₂ [†]	22.8 (1)	37.7 (1)
Amorphous	40.5 (2)	62.2 (3)
Total	99.9	99.9
R _{wp} (%)	2.85	3.46
R _p (%)	2.58	2.72
χ ²	1.98	2.11

[†]The structures have tetragonal *P4₂/nmc* symmetry.

Table II. Structural and Physical Properties of Powders

Sample	Average diameter (nm) BET	Average diameter (nm) XRD	d ₁₁₁ (nm) XRD
Zr0	8.5	<i>m</i> -phase: 12 <i>t</i> -phase: 11	0.295
Zr10	6.7	7.9	0.298

XRD, X-ray diffraction.

determined by BET. The differences between the average crystallite size as determined by X-ray line broadening and TEM image analysis (Fig. 2), and the average grain size obtained by specific surface area analysis are evidence of light grain agglomeration.

In Fig. 3, the weight loss and the differential thermal analysis curves up to 1200°C are reported. The observed weight loss is due, in addition to both chemically coordinated and physisorbed water, to residual oxo-bridging and non-bridging structural hydroxyl group and it is a sign of the crystallization degree of the powders. The DTA curve exhibits, at about 70°C, the endothermic peak characteristic of water elimination and around 420°C, a weak exothermic peak. The sharp endothermic peak near 1200°C corresponds to the equilibrium transition *m*- to *t*-ZrO₂, whose reversibility is confirmed by the exothermic signal observed near 900°C in the cooling curve.

Relative fractions of the different hyperfine components obtained in the fitting procedure of the PAC spectra have been plotted in Fig. 4. At room temperature the powder composition is 68% of *t'*, 5% of *t*-phase, and 27% of a very disordered *m*-phase, indicating that pure zirconia has partially stabilized in the tetragonal phase. As the temperature increases, the *t'* configurations transform to both, the more regular and crystalline *t*-phase, which achieves its maximum concentration at 400°C, and the monoclinic phase, whose relative fraction shows a permanent increase with temperature. At 600°C, the conversion of the tetragonal polymorphs to monoclinic zirconia is manifest.

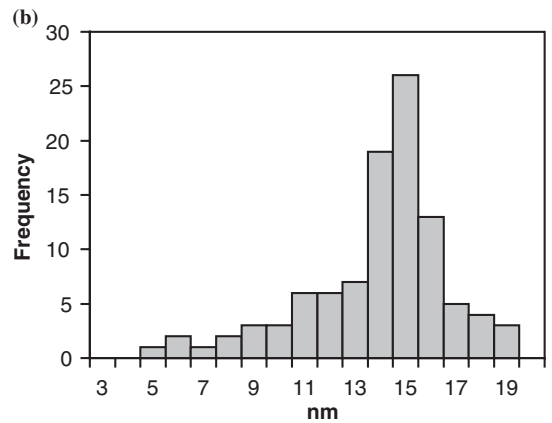
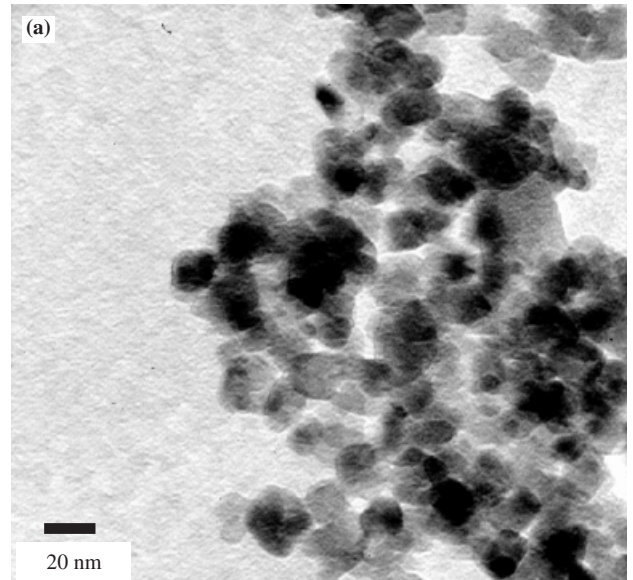


Fig. 2. Transmission electron micrograph of Zr0 sample (a) and grain size distribution obtained by image analysis (b).

(2) Doped Zirconia (Zr10)

As shown in Fig. 5, the as-obtained doped product is a finely divided powder of quite stabilized tetragonal zirconia. Also in this case an unambiguous determination of the crystal structure cannot be made solely from XRD results. Moreover, the quantitative analysis performed by the Rietveld-RIR method shows

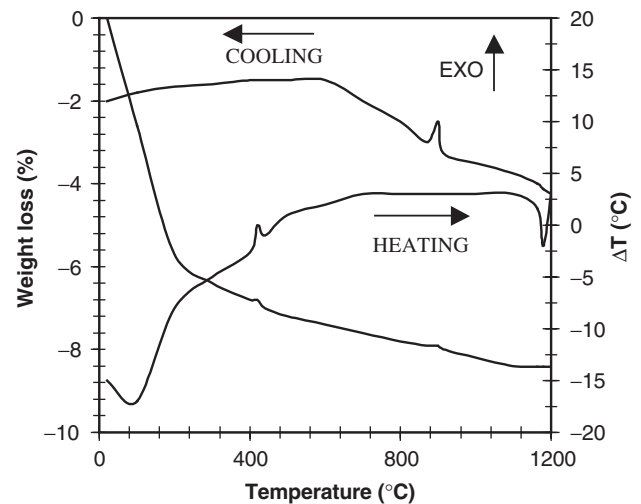


Fig. 3. Thermogravimetric and differential thermal analysis curves of Zr0 sample.

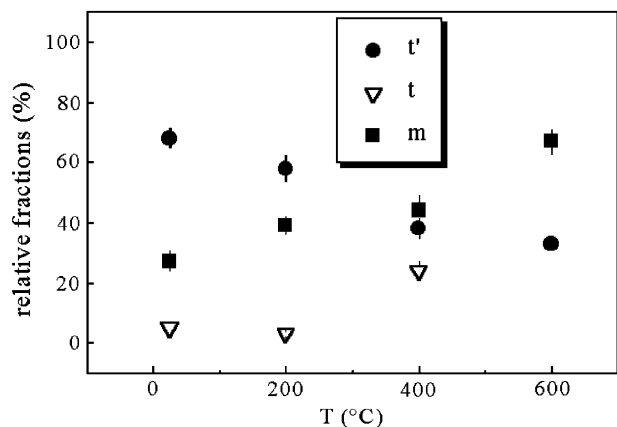


Fig. 4. Perturbed angular correlation relative fractions of ZrO as a function of temperature.

the presence of an amorphous X-ray phase (see Table I). The shift of the tetragonal diffraction line toward lower angles as compared with pure zirconia indicates that praseodymium doping causes an increase in the interplanar spacing (shown in Table II) and consequently in the cell dimensions. Table II also reports the average grain size determined by both BET values and XRD pattern analysis. The obtained results match with TEM results obtained on this sample, contained in Fig. 6, indicating well-dispersed particles.

TG and DTA curves up to 1200°C are reported in Fig. 7. The TG behavior is very similar to ZrO sample evidencing the uncompleted crystallization of the starting product. The DTA curve shows, near 80°C, the endothermic signal characteristic of water elimination and at around 480°C, an exothermic signal. At higher temperatures, the DTA curve indicates the thermal stability of the synthesized powders. Nevertheless, a subtle baseline change can be observed at 900°C on heating and cooling. A new diffractogram (Fig. 8(a)) obtained after the DTA experiment up to 1200°C allows to distinguish the stabilized zirconia polymorph. In fact, an inspection of region 72°–76° (Fig. 8b) reveals that the Pr addition stabilizes the tetragonal structure.²⁵ In fact, the high-angle region pattern shows the splitting of the (400) and (004) reflections characteristic of a tetragonal phase (otherwise, the cubic phase only presents the (004) reflection in this region).

Figure 9 shows the thermal evolution of the relative fractions of the hyperfine interactions fitted. In agreement with the XRD data, PAC results indicate that the product obtained under the microwave-hydrothermal synthesis is completely stabilized in the tetragonal phase, indicating, in addition, that it is depicted by the defective and disordered tetragonal *t'*-form. Up to 400°C, only the *t'*-ZrO₂ phase is present. At 600°C, a small amount of the crystalline *t*-ZrO₂ phase appears. At 800°C, an additional

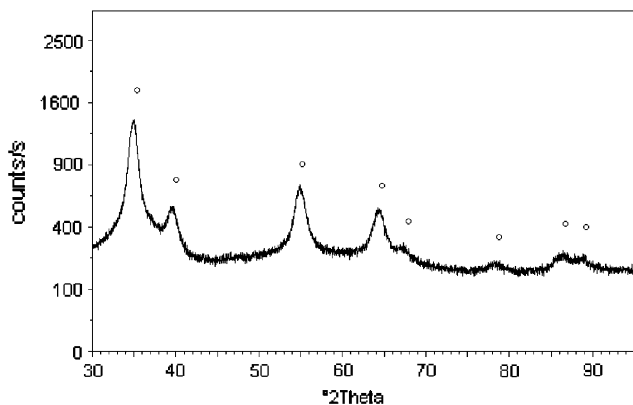


Fig. 5. X-ray diffraction pattern of as-obtained Zr10 sample. °, *t*-ZrO₂.

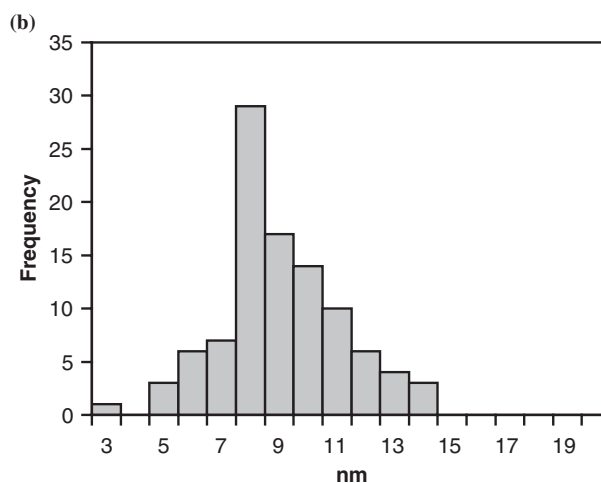
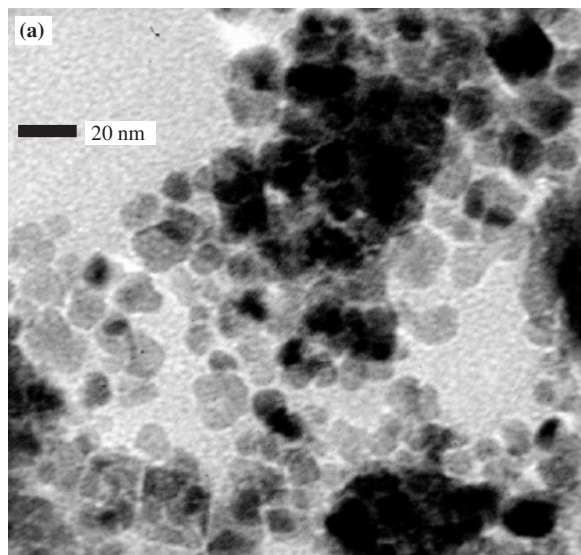


Fig. 6. Transmission electron micrograph of Zr10 sample (a) and grain size distribution obtained by image analysis (b).

unknown interaction, hereinafter called X, becomes necessary to obtain a satisfactory fit. As temperature increases up to 1150°C, PAC results indicate that the *t*-phase and the configuration described by the X-interaction grow at the expense of the *t'*-phase.

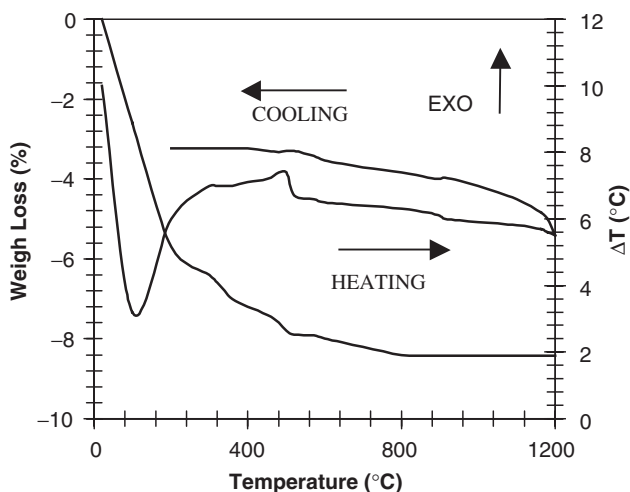


Fig. 7. Thermogravimetric and differential thermal analysis curves of Zr10 sample.

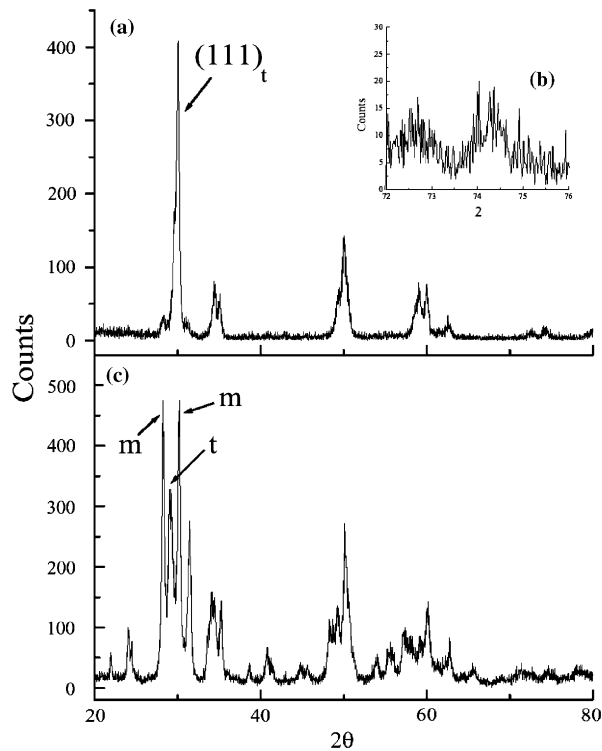


Fig. 8. X-ray diffraction pattern of Zr10 sample after differential thermal analysis (DTA) analysis (a), selected 72° – 76° angular region after DTA analysis (b) and X-ray diffraction pattern after perturbed angular correlation measurements (c).

The cooling from 1150°C to room temperature causes a partial degradation of the sample, yielding 43% of $m\text{-ZrO}_2$, 16% of t -form, and 41% of t' -form. No X-form is present. A final XRD experiment performed on the activated sample used for the PAC experiment reproduced this result, as can be observed in Fig. 8(c).

IV. Discussion

Pure zirconia synthesized by the microwave-hydrothermal method become partially stabilized. Particle size obtained from different techniques on this sample indicates that stabilization has proceeded by a size effect. Moreover, TG/DTA information and the quantitative results obtained by the Rietveld-RIR method suggests that the crystallization of the obtained powders is not completed under the present synthesis conditions. Although there might be OH-free domains of $t\text{-ZrO}_2$, the as-obtained

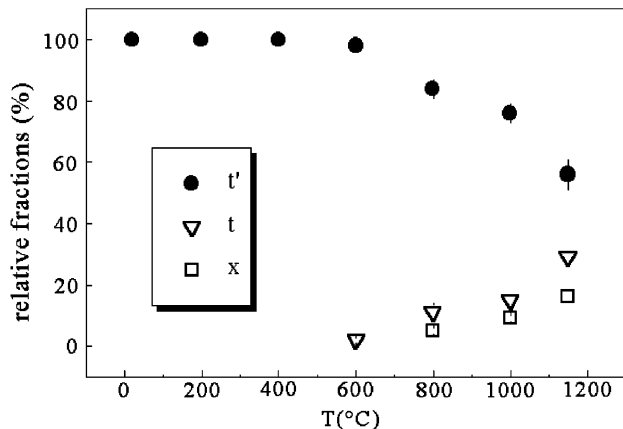
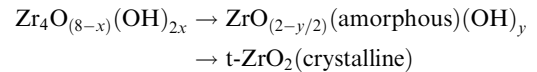


Fig. 9. Perturbed angular correlation relative fractions of Zr10 as a function of temperature.

sample still has many OH (see the TG curve), probably in residual amorphous regions whose atomic structure is undetectable by XRD analysis. The exothermic peak present in the DTA curve at 420°C must be considered as being a result of the crystallization of the residual amorphous phase. This thermal change, observed at 480°C for Zr10, confirms that the crystallization temperature increases with the addition of praseodymium,¹⁴ and it is correlated with a weight loss matching to the thermal dehydroxylation pathway:



characteristic of precipitated samples.²⁶

The atomic-scale PAC information allows reporting that the starting powder is predominantly in the defective and disordered tetragonal t' -phase. This fact justifies the assumption that the structure of the amorphous phase is tetragonal-like, as it has been suggested by other authors on the basis of X-ray radial distribution²⁷ and X-ray diffraction data.²⁸ As temperature is increased, the crystallization occurs and the t' -phase gradually transforms into the more regular tetragonal structure and monoclinic phase. While the former structure shows a drastic increase of its relative fraction near the temperature of the DTA exothermic peak, the latter grows continuously with temperature, indicating the irreversible degradation of the ceramic. Accordingly, at temperatures higher than 600°C , DTA reveals that the powder evolves as ordinary pure zirconia.

Concerning the powder doped with 10% of praseodymium, XRD indicates that the resulting microwave-hydrothermal product is wholly stabilized. A comparison with XRD information obtained on the undoped sample allows to state that this difference is due to the presence of additional oxygen vacancies created by the substitutional replacement of Zr cations by Pr cations. This localization of the dopant cations is coherent with the shift of the diffraction lines toward lower angles.

PAC characterization, in turn, evidenced that the stabilization led to 100% of tetragonal zirconia in its t' -phase, this defective structure now including, in addition, the oxygen-defective atomic configurations produced for charge balance inherent to substitutional Pr replacements. The thermal transformation between the disordered t' - and the ordered t -phases that occurred between 400° and 600°C can be associated to hydroxyl removal. The second change, from t' -phase to X-form, is observed at 800°C . Regarding the last interaction, based on the subtle reversible DTA signal at 900°C and on results concerning structural changes in stabilized zirconias, it has been assumed that it corresponds to a metastable cubic structure. In fact, Bouc'h *et al.*²⁹ have reported that in some sesquioxide- ZrO_2 nanostructured solid solutions, a step in the base-line reflecting the second-order $t \rightarrow c$ transition was observed for dopant concentrations higher than 2.5 mol%. Moreover, Withers *et al.*³⁰ have reported, for the same composition as ours, the existence of a "defect fluorite-type" cubic solid solution in an equilibrium situation at higher temperatures.

Concerning the thermal stability of the doped phase, it can be observed that the relevant amount of monoclinic phase determined by PAC after cooling from 1150°C , also revealed by the diffractogram of Fig. 8(c) obtained on the same active sample, is not present in the diffractogram shown in Fig. 8(a). This controversial result can be explained considering the different heating treatments inherent to both experiments. It is evident that the time used for the DTA analysis, much shorter than the duration of each PAC experiment, was not enough to degrade the stabilized zirconia solid solution.

V. Conclusions

Microwave-assisted hydrothermal synthesis has proved to be a very suitable environmentally friendly processing method for the synthesis of praseodymium-doped (Pr = 10 mol%) zirconia

powders. It improves the powder quality and allows to produce stabilized tetragonal zirconia with relatively high crystallinity.

The PAC technique enabled the determination of a tetragonal-like structure for the XRD-determined amorphous fractions in the starting products. In particular, the possibility of performing the hyperfine experiments as a function of temperature allowed an *in situ* investigation on the thermal pathway of the microwave-hydrothermal-synthesized zirconia.

The obtained results, compared with the TG/DTA curves and with the quantitative Rietveld-RIR results, allowed to define as the exothermic peak, present in both the investigated samples, respectively, at 420° and 480°C, is to attribute to the crystallization of the residual XRD amorphous phase that at atomic scale, as determined by PAC, transforms from the defective and disordered *t'*-ZrO₂ into the more regular *t*-ZrO₂. The predominance of the defective *t'*-form over the whole thermal range investigated and the shift of the diffraction lines towards lower angles are consistent with the localization of Pr ions at substitutional Zr sites.

Acknowledgments

The authors are grateful to Dr. Daniele Verucchi, who performed the experimental procedure and Dr. Paola Miselli for assistance in XRD diffraction analysis.

The S&T cooperation 1999–2000 between Italy (Ministero degli Affari Esteri) and Argentina (SETCIP-MAE) project (IT.12/99) is gratefully acknowledged.

References

- ¹T. Sugimoto (Ed.) *Fine Particles: Synthesis, Characterisation and Mechanism of Growth*. Marcel Dekker, New York, NY, 2000.
- ²S. Somyia and T. Akiba, "Hydrothermal Zirconia Powders: A Bibliography," *J. Eur. Ceram. Soc.*, **19**, 81–7 (1999).
- ³S. Somyia, M. Yoshimura, Z. Nakai, K. Hishinuma, and T. Kumaki, "Synthesis of ZrO₂ and TiO₂ nano-crystalline powders by hydrothermal process"; pp. 465–74 in *Microstructure*, Edited by J. A. Pask, and A. Evans. Plenum Press, New York, 1986.
- ⁴T. Tsukada, S. Venigalla, A. A. Morrone, and J. H. Adair, "Low-Temperature Hydrothermal Synthesis of Yttrium-doped Zirconia Powders," *J. Am. Ceram. Soc.*, **82** [5] 1169–74 (1999).
- ⁵S. Komarneni, R. Roy, and Q. H. Li, "Microwave-Hydrothermal Synthesis of Ceramic Powders," *Mater. Res. Bull.*, **27** [12] 1393–405 (1992).
- ⁶S. Komarneni, "Novel Microwave-Hydrothermal Processing for Synthesis of Ceramic and Metal Powders"; pp. 103–17 in *Novel Techniques in Synthesis and Processing of Advanced Materials*, Edited by J. Singh, and S. M. Copley. The Minerals, Metals and Materials Society, Warrendale, PA, 1995.
- ⁷S. Komarneni, M. C. D'Arrigo, C. Leonelli, G. C. Pellacani, and H. Katsuki, "Microwave-Hydrothermal Synthesis of Nanophase Ferrites," *J. Am. Ceram. Soc.*, **88** [11] 3041–4 (1998).
- ⁸F. Bondioli, C. Leonelli, C. Siligardi, G. C. Pellacani, and S. Komarneni, "Microwave and Conventional Hydrothermal Synthesis of Zirconia Doped Powders;" in *Advances in Microwave and Radio Frequency Processing*, Edited by M. Willert-Porada. Springer Verlag, Berlin, 2003 in press.
- ⁹F. Bondioli, A. M. Ferrari, C. Leonelli, C. Siligardi, and G. C. Pellacani, "Microwave-Hydrothermal Synthesis of Nanocrystalline Zirconia Powders," *J. Am. Ceram. Soc.*, **84** [11] 2728–30 (2001).

- ¹⁰C. J. Howard, R. J. Hill, and B. E. Reichert, "Structures of the ZrO₂ Polymorphs at Room Temperature by High-Resolution Neutron Powder Diffraction," *Acta Crystallogr.*, **B 44**, 116–20 (1988).
- ¹¹R. Ramamoorthy, D. Sundararaman, and S. Ramasamy, "X-ray Diffraction Study of Phase Transformation in Hydrolyzed Zirconia Nanoparticles," *J. Eur. Ceram. Soc.*, **19**, 1827–33 (1999).
- ¹²C. K. Narula, J. E. Allison, D. R. Bauer, and H. S. Gandhi, "Materials Chemistry Issues Related to Advanced Materials Applications in the Automotive Industry," *Chem. Mater.*, **8** [5] 984–1003 (1996).
- ¹³A. D. Logan and M. Shelef, "Oxygen Availability in Mixed Cerium/Praseodymium Oxides and the Effect of Noble Metals," *J. Mater. Res.*, **9** [2] 468–75 (1994).
- ¹⁴A. Bonamartini Corradi, F. Bondioli, and A. M. Ferrari, "Role of Praseodymium on Zirconia Phases Stabilization," *Chem. Mater.*, **13**, 4550–4 (2001).
- ¹⁵N. Mommer, T. Lee, J. A. Gardner, and W. E. Evenson, "Oxygen Vacancy Trapping in Tetragonal ZrO₂ Studied by ¹¹¹In/Cd Perturbed Angular Correlation," *Phys. Rev. B*, **61**, 162–7 (2000-1).
- ¹⁶P. C. Rivas, M. C. Caracoche, A. F. Pasquevich, J. A. Martínez, A. M. Rodríguez, A. R. López García, and S. R. Mintzer, "Characterization of Metastable Tetragonal Forms in ZrO₂-2.8% Y₂O₃ Ceramics," *J. Am. Ceram. Soc.*, **79**, 831–36 (1996).
- ¹⁷R. Caruso, E. Benavidez, O. de Sanctis, M. C. Caracoche, P. C. Rivas, M. Cervera, A. Caneiro, and A. Serquis, "Phase Structure and Thermal Evolution in Coatings and Powders Obtained by the Sol-Gel Process: Part II. ZrO₂-2.5 mole% Y₂O₃," *J. Mater. Res.*, **12** [10] 2594–601 (1997).
- ¹⁸A. M. Rodríguez, M. C. Caracoche, P. C. Rivas, A. F. Pasquevich, and S. R. Mintzer, "PAC Characterization of Nontransformable Tetragonal *t'* Phase in Arc-Melted Zirconia-2.8 mol% Ytria Ceramics," *J. Am. Ceram. Soc.*, **84** [1] 188–92 (2001).
- ¹⁹P. C. Rivas, M. C. Caracoche, J. A. Martínez, A. M. Rodríguez, R. Caruso, N. Pellegrini, and O. de Sanctis, "Phase Structure and Thermal Evolution in Coatings and Powders Obtained by the Sol-Gel Process: Part I. ZrO₂-11.3 mole% Y₂O₃," *J. Mater. Res.*, **12** [2] 493–9 (1997).
- ²⁰Powder Diffraction File, Card 37-1484, International Centre for Diffraction Data, Newtowne Square, PA, 1995.
- ²¹Powder Diffraction File, Card 42-1164, International Centre for Diffraction Data, Newtowne Square, PA, 1995.
- ²²A. C. Larson and R. B. Von Dreele in *GSAS: General Structure Analysis System LANSCE, MS-H805*. Los Alamos National Laboratory Report, 86-748 (2000).
- ²³H. M. Rietveld, "Profile Refinement Method for Nuclear and Magnetic Structures," *J. Appl. Crystallogr.*, **2**, 65–71 (1969).
- ²⁴*Elements of X-ray Diffraction*, 2nd edition, Edited by B. D. Cullirry. Addison-Wesley, Reading, MA, 1997.
- ²⁵M. Sugiyama and H. Kubo, "Microstructure of the Cubic and Tetragonal Phases in a ZrO₂-Y₂O₃ Ceramic System;" pp. 965–73 in *Advances in Ceramics Vol. 24B, Science and Technology of Zirconia III*, Edited by S. Somyia, N. Yamamoto, and H. Yanagida. American Ceramic Society, Westerville, OH, 1988.
- ²⁶A. V. Chadwick, G. Mountjoy, V. M. Nield, I. J. F. Poplett, M. E. Smith, J. H. Strange, and M. Tucker, "Solid-state NMR and X-ray Studies of the Structural Evolution of Nanocrystalline Zirconia," *Chem. Mater.*, **13**, 1219–29 (2001).
- ²⁷O. Stachs, T. Gerber, and V. Petkov, "Atomic-Scale Structure of ZrO₂ Xerogels by X-ray Diffraction and Reverse Monte Carlo Simulations," *J. Non Cryst. Solids*, **210** [1] 14–21 (1997).
- ²⁸R. Gomez, T. López, X. Bokhimi, E. Muñoz, J. L. Boldú, and O. Novaro, "Dehydroxylation and the Crystalline Phases in Sol-Gel Zirconia," *J. Sol-Gel Sci. Technol.*, **11** [3] 309–19 (1998).
- ²⁹F. Boule'h and E. Djurado, "Structural Changes of Rare-Earth Doped Nanostructured Zirconia Solid Solution," *Solid State Ionics*, **157** [1–4] 335–40 (2003).
- ³⁰R. L. Withers, J. G. Thompson, P. J. Barlow, and J. C. Barry, "The "Defect Fluorite" Phase in the ZrO₂-PrO_{1.5} System and its Relationship to the Structure of Pyrochlore," *Austral. J. Chem.*, **45**, 1375–95 (1992). □